

Hot-press sintering of Ge-Si alloys

N. SAVVIDES*, H. J. GOLDSMID

Department of Applied Physics, University of New South Wales, Kensington 2033, Australia

Germanium-silicon alloys of the composition $\text{Ge}_{30}\text{Si}_{70}$ have been prepared by hot pressing powder compacts at temperatures between 1300 and 1493 K (the solidus temperature) at pressures up to 40 MPa. The densification of the compacts was observed as a function of time. For each temperature and pressure an end-point density less than the full density was found. The time-dependence of the densification and the pressure-dependence of the end-point density can be described empirically in terms of a plastic flow mechanism.

1. Introduction

Germanium-silicon alloys have been established for some years as favourable thermoelectric materials for use at high temperatures [1, 2]. Recently, radioisotopic power generators, based on these alloys, capable of delivering hundreds of watts, have been developed to provide onboard power for deep-space missions (1977 Jupiter-Saturn Mariner spacecraft) and for use in the US Air Force communication satellite launched in 1976 [3, 4].

The use of heavily doped Ge-Si alloys suitable for thermoelectric applications has been exhaustively treated both experimentally [1, 5-7] and theoretically [8-10]. These treatments were essentially on single-crystal or large-grain polycrystal materials which were prepared by the zone levelling technique [11], under rigidly controlled conditions [12]. In device application, material cost is a significant factor and the preparation of large quantities of material by zone levelling prohibits the establishment of a cheap technology. Thus, in the last decade, great interest has been shown in the use of hot-pressing methods for large scale preparation of these alloys; the hot-pressing process affords considerable saving in materials and cost and facilitates thermoelectric module construction. Despite the technological importance of the hot-pressing process, however, fundamental information has not appeared in literature concerning the factors that affect and

control the process. Such information, we feel, is of great importance since, in sintered fine-grained Ge-Si alloys, the possibility exists of improving the thermoelectric figure of merit by making use of the effect of phonon boundary scattering [13-16].

A number of authors have described methods of hot pressing Ge-Si alloys. Huffadine [17] produced $\text{Ge}_{15}\text{Si}_{85}$ by hot pressing at temperatures between 1620 and 1670 K that are well above the solidus temperature for this alloy, 1580 K, and achieved high densities through the liquid filling of interstices. Rowe and Bunce [18-20] have prepared alloys of similar composition, again pressing at high temperatures and almost certainly obtaining high densities through the presence of the liquid phase. Lefever *et al.* [21] used a high pressure, 193 MPa, in the hot pressing of $\text{Ge}_{20}\text{Si}_{80}$ to within about 1% of maximum density. Sahn and Gnau [22] also used high pressures, between 170 and 340 MPa, at temperatures just below that of the solidus, to produce $\text{Ge}_{37}\text{Si}_{63}$; 94% of maximum density was reached with homogeneous starting materials while up to 99.5% of maximum density was observed for inhomogeneous alloys. Undoubtedly, a Ge-rich liquid phase was present in the inhomogeneous materials.

In our experiments we were primarily concerned with establishing the effect of grain size on the lattice thermal conductivity [23]. Since free carrier scattering of phonons is known to

*Present address: Department of Physics, Electronics and Electrical Engineering, U.W.I.S.T., Cardiff, UK.

compete more or less directly with boundary scattering in decreasing lattice thermal conductivity [10], we avoided the high concentration of doping impurities that are essential to a high thermoelectric figure of merit. In order to control grain size during hot pressing, we prepared alloys which had little variation in alloy composition, and we hot pressed at temperatures below the solidus temperatures so as to eliminate the substantial grain growth and recrystallization that inevitably occurs whenever a liquid phase is present. The observations on the densification processes that are described here were for Ge₃₀Si₇₀ alloy (30 at.% Ge, 70 at.% Si); at this composition the solidus temperature is 1493 K.

2. Experimental details

2.1. Preparation of alloys

Germanium and silicon are miscible in all proportions forming a binary phase system [24]. To produce bulk quantities of any one alloy composition from the melt would require an immediate quench of the entire melt through the liquidus–solidus zone. The wide separation between liquidus and solidus, combined with the low thermal conductivity of the alloys, can result in severe alloy segregation in chill cast ingots. In addition, the low diffusion coefficient of the component elements in the solid ($\sim 10^{-12}$ cm² sec⁻¹) makes it impossible to homogenize chill-cast ingots by annealing [24]. Completely homogeneous alloys, that is alloys in which the distribution of the chemical elements is uniform on an atomic scale, are usually prepared by the zone levelling technique [12]. However, for reasons outlined earlier, alternative methods for preparing alloys are needed. Conventional chill-casting methods whereby a large quantity of molten alloy is cast in water-cooled copper moulds, have been used in the past and were shown to result in ingots varying by up to 50% in alloy composition [25].

The materials used in our experiments were large-grain polycrystal ingots, approximately 2 cm diameter and 50 to 80 g weight, prepared by a rapid quenching technique [23]. The charge materials were high purity Ge and Si supplied by Johnson Matthey Metals (London); typical impurities were Ca, Mg, Fe and Cu of concentration \leq 1 ppm. The structure of the ingots (see [26] for definition) was determined by measuring density

and thermoelectric power of different sections of each ingot, and by examining homogeneity by employing optical microscopy and scanning electron microscopy (SEM) techniques. The density of sections of ingots was determined by the method of hydrostatic weighing employing Archimedes' principle [27]. The density values obtained were in good agreement with published data on zone levelled materials [28]. Measurement of the thermoelectric power, by scanning the surface of the specimens with a Seebeck hot probe [29, 30] did not reveal any obvious large scale segregation. Microscopy techniques, however, indicated the presence of microscale inhomogeneities; alloy segregation took place at the grain boundaries due to solute rejection upon solidification. The observed grain structure was cellular–dendritic typical of chill-cast alloys. A quantitative estimate of the degree of inhomogeneity was obtained using SEM by employing atomic number contrast techniques; atomic number contrast results from specimens that contain regions of elements with differences in atomic number [31]. If all other factors contributing to contrast are equivalent from the low and high atomic number regions, the resulting contrast can be used to identify alloy phases. In our technique, a normal image of the test specimen was obtained, and then the SEM was operated in the single scan mode and a record made of the collector intensity as the electron beam was made to travel slowly across a line on the specimen. The signal level is proportional to atomic number and hence density, and thus it is possible to obtain a record of the density profile along a line intersecting several grains and boundaries. Similar signals were obtained from single crystal specimens of Si and Ge and used to calibrate the density scale. This scale can then be converted to a scale of alloy composition from the known variation of density with composition. The result of these studies indicated that grains had a uniform composition and that the grain boundaries were richer in Ge by up to 5%. The amount of Ge-rich material involved at grain boundaries was small and estimated to be of the order of a few percent. Our conclusions from these studies are that the ingots solidified with a major phase (that of grains) which is very close to the nominal composition and with very little Ge-rich material rejected at the grain boundaries. The materials are thus suitable for the hot-pressing method and for our purposes they may be described as homogeneous.

2.2. Production of powders

The ingots were reduced to powders which were then classified into distinct size ranges of uniform grain size distributions. In the first stage, each ingot was reduced to coarse powder of $\leq 100 \mu\text{m}$ diameter using an agate pestle and mortar. Further reduction was carried out by planetary ball milling in agate vessels of volume 3 cm^3 using agate balls. McVay *et al.* [32] reported that Ge-rich alloys are easier to reduce than Si-rich alloys and thus if a long time is spent in milling and the ingot is not completely homogeneous the process yields fine powders which are rich in Ge and coarse powders which are rich in Si. To avoid this problem, we have restricted milling times to 10 to 30 sec and milled small amounts (0.5 g) of powder at a time. The result was discontinuous reduction producing mostly powders of 40 to $20 \mu\text{m}$. During screening, powders were returned for further milling till all powder produced was $40 \mu\text{m}$ to about $1 \mu\text{m}$.

Agate was chosen as a milling material since it is more abrasive than most other materials usually used in milling and it is known to introduce the least amount of impurities [32]; the main added impurity is SiO_2 which is already present to some extent in our materials. We found that after the first grind, the agate tools became coated with the material being ground thus preventing excessive contamination.

In the second stage, the reduced powders were classified into distinct size ranges by screening successively through five sieves. The sieves were Endecott sieves with circular perforations of diameters 40, 30, 22, 15 and $10 \mu\text{m}$. To facilitate sifting, powders were dispersed with ethanol. Powders of diameters $\leq 10 \mu\text{m}$ were classified into sizes of 10 to $4 \mu\text{m}$ and 4 to $0.5 \mu\text{m}$ by collecting settled powders.

Detailed studies reported in this paper were carried out on two ranges of size, namely $-40+30 \mu\text{m}$ and $-15+10 \mu\text{m}$; the terminology used here is a negative sign to indicate powder passing through one sieve and a positive sign for powder stopped by the next sieve. An examination of grain size and shape was undertaken employing optical and SEM techniques. Representative samples from each size range showed a uniform distribution in grain size. The shape of grains was that of irregular polyhedra with sharp corners and edges with highly reflecting faces indicating cleavage from single crystals of larger dimensions.

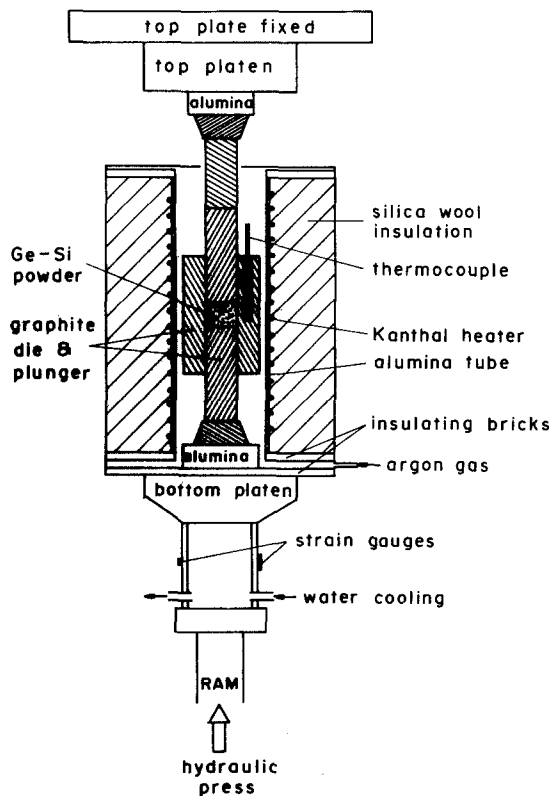


Figure 1 Arrangement for hot pressing of Ge-Si powders.

2.3. Hot pressing

The hot pressing of compacts was carried out in a graphite die that was heated by a Kanthal heater. The die assembly is shown in Fig. 1. A flow of pure argon gas was maintained in the furnace throughout the process. Pressure was applied by means of a hydraulic press, the pressure being monitored by strain gauges to an accuracy of $\pm 0.4 \text{ MPa}$. The graphite die set a pressure limit of 40 MPa . The compacts were 26 mm diameter and 3 to 5 mm thick; the high ratio of diameter to thickness ensured uniform pressure distribution and density [33].

The density of each compact was determined from its weight and dimensions. Each compact was first ground to a uniform thickness. The weighing was done with a Mettler H20 balance of 10^{-5} g rated sensitivity. A precision micrometer was used to measure diameter and thickness obtaining average values for these dimensions. The error of determining density was about 0.3%. The relative density was obtained from the ratio of the density of each compact to that of the parent ingot. When this ratio is unity the compact is said to have attained theoretical density.

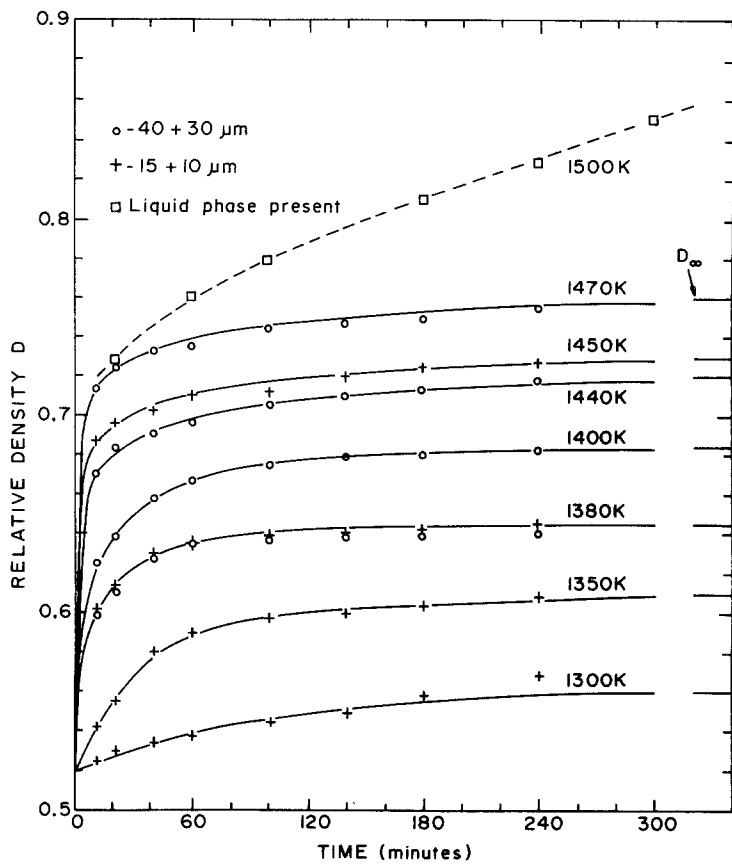


Figure 2 Plots of relative density against time for various temperatures at a pressure of 30 MPa. The solid curves satisfy Equation 1.

3. Experimental results

Fig. 2 shows how the relative density was observed to vary with time for various sintering temperatures and a pressure of 30 MPa. Results are given for both the ranges of powder size that were employed. The diagram also shows the behaviour when the temperature was raised above the solidus temperature T_S ; the presence of a liquid phase very

obviously leads to appreciably higher densities and a very different variation of density with time.

It can be seen that the plots are all approaching an end-point relative density D_∞ that rises with increasing temperature. End-point densities were determined at other pressures so that the variation of D_∞ with pressure P could also be found. The results are given in Fig. 3 for these typical tem-

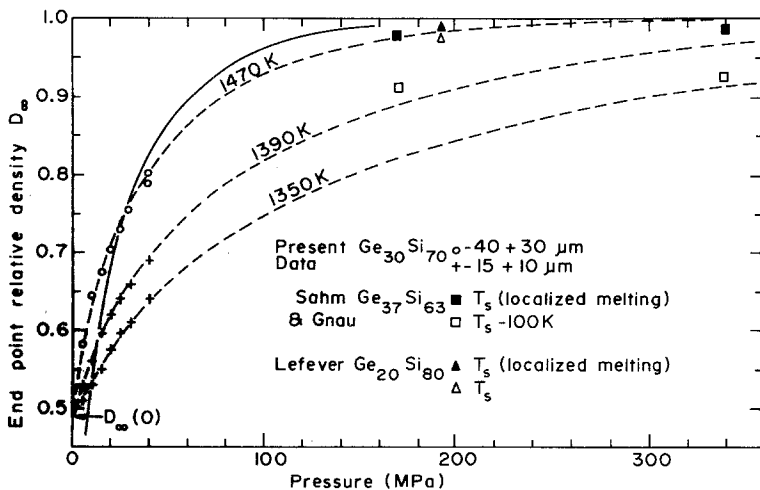


Figure 3 Plots of end-point relative density against pressure at various temperatures. The broken curves satisfy Equation 3 and the solid curve is based on Equation 2.

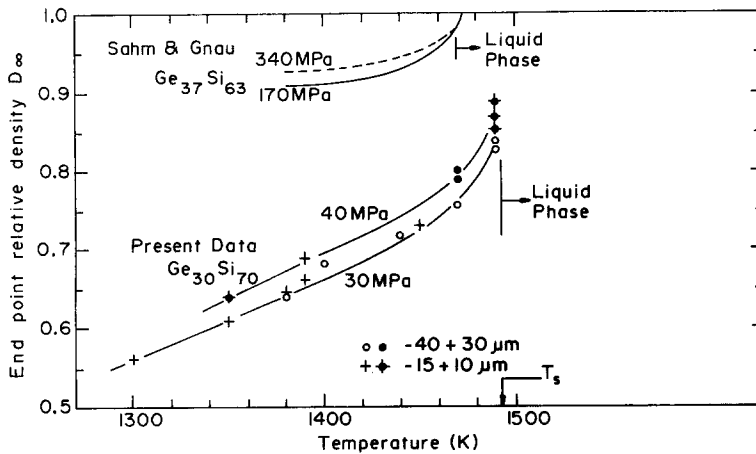


Figure 4 Plots of end-point relative density against temperature.

peratures. Also shown are the data of Sahm and Gnau [22] and Lefever *et al.* [21] obtained for somewhat different compositions at much higher pressures.

Finally, the variation of end-point relative density with temperature T is shown in Fig. 4. It is seen that D_∞ varies linearly with T below about 1460 K but at higher temperatures the plots show an upward curvature as T_S is approached. Sahm and Gnau observed a somewhat similar behaviour at very much higher pressures.

4. Discussion

The experimental results do not reveal any significant dependence on the size of the powder particles. They indicate an initial relative density of 0.52 with end-point relative densities D_∞ varying from 0.56 to 0.76. In all cases a very rapid initial rate of densification was followed by a much slower rate and (except when a liquid phase was present) the rate of densification became almost imperceptible after 5 h.

In attempting to find a sintering mechanism that is consistent with the observed behaviour we have considered densification by diffusion and by plastic flow. It appears that neither lattice nor boundary diffusion can explain the relatively high rate of densification for powders of the size that we have employed. Thus, we think that a plastic flow mechanism is appropriate.

A model based on plastic flow was proposed by Mackenzie and Shuttleworth [34] and extended to hot pressing by McClelland [33]. The Mackenzie-Shuttleworth mechanism assumes that the pores are isolated spheres and that normal sintering takes place under the influence of surface tension. McClelland showed that, during hot

pressing, the pressure acts as an additional surface tension [35]. Thence it is found that the rate of densification for high pressures is

$$\frac{dD}{dt} = K\phi \left(\frac{1}{1-\phi^2} + a \ln \phi \right) \quad (1)$$

where $K = 3P/4\eta$, P being the pressure and η the viscosity at infinite shear strain, ϕ is the porosity defined as $(1-D)$, and $a = \sqrt{2}\tau_c/P$, τ_c being the critical shear stress.

From Equation 1 we expect the end-point porosity ϕ_∞ , equal to $1 - D_\infty$, to be given by

$$(1 - \phi_\infty^2) \ln(1/\phi_\infty) = P/\sqrt{2}\tau_c. \quad (2)$$

The end-point relative density D_∞ can be less than unity and we expect it to be pressure-dependent and also temperature-dependent since the critical yield stress τ_c is itself temperature-dependent.

The solid curves, shown in Fig. 2, satisfy Equation 1 and fit the experimental data remarkably well, if suitable values of η and τ_c are chosen, as given in Table I. Although we do not know the true values of η and τ_c for Ge-Si alloys, the variation of the quantities as $\exp(-BT)$ is as expected and there is agreement with the general

TABLE I Variation of yield stress τ_c and viscosity η with temperatures at pressure 30 MPa

Temperature (K)	τ_c (MPa)	η (10^{10} Nsec m^{-2})
1300	61	75
1350	48	25
1380	41	7.5
1400	34	5.6
1440	29	2.4
1450	28	1.9
1470	24	1.1

behaviour of germanium and silicon observed by Patel and Chaudhuri [36].

Knowing the critical shear stress as a function of temperature, one should be able to relate D_∞ to P using Equation 2. However, this equation predicts that D_∞ should be zero when P is zero, whereas the results shown in Fig. 3 indicate that the zero-pressure value of D_∞ is 0.49. The solid curve in Fig. 3 is based on the value of $\tau_c = 24$ MPa obtained from our observations at a pressure of 30 MPa and a temperature of 1470 K and obviously does not fit the results very well.

Equation 2 can be improved in the following empirical fashion. It is supposed that there is an effective pressure P_0 that acts on the pores leading to a finite end-point relative density $D_\infty(0)$ when no external pressure is applied. Now Equations 1 and 2 were derived on the basis that the pressure on the pores is $P/(1 - \phi^{2/3})$, so we must replace this quantity by $P/(1 - \phi_\infty^{2/3}) + P_0$. If we do this, we obtain

$$\{\ln(1/\phi_\infty) - \ln(1 - \phi_0)\}(1 - \phi_\infty^2) = P/\sqrt{2}\tau_c \quad (3)$$

where $\phi_\infty = 1 - D_\infty(0)$. The experimental data show that $\phi_0 = 0.51$. In effect, P_0 may be regarded as an approximation to the surface tension term of Mackenzie and Shuttleworth.

The broken lines in Fig. 3 correspond to Equation 3 with only τ_c as an adjustable parameter and fit the data well at all temperatures. They indicate end-point relative densities of the order of those found by Sahm and Gnau [22] and by Lefever *et al.* [21] for high pressures, though we should remember that these authors used somewhat different alloy compositions from ours.

Some support for the assumption of a plastic flow mechanism was obtained from examination of the fractured surfaces of several compacts using optical and scanning electron microscopy. It was observed that the grain size in the compacts was similar to that of the starting powders and that there was little change of shape other than rounding at the intergranular contacts for high pressures and temperatures. This rounding effect is strong evidence for plastic flow while an observation that the grain boundaries remain at the interparticle necks suggests that diffusion mechanisms are unimportant. However, residual interconnection of the pores, even at high densification, shows that the Mackenzie–Shuttleworth model cannot fully describe the real structure of the compacts.

5. Conclusions

This work which forms what is probably the first systematic study of the effects of pressure and temperature on the sintering of Ge–Si alloys, suggests that densification occurs by means of a plastic flow mechanism. The behaviour is consistent with an empirical model derived from the Mackenzie–Shuttleworth–McClelland theory, but further work must be done before the details of the sintering process can be established.

Acknowledgements

The authors acknowledge the support of the Australian Research Grants Committee.

References

1. J. P. DISMUKES, L. EKSTROM, E. F. STEIGMEIER, I. KUDMAN and D. S. BEERS, *J. Appl. Phys.* **35** (1964) 2899.
2. F. D. ROSI, *Solid State Electronics* **11** (1968) 833.
3. C. E. KELLY, Proceedings of the 10th Intersociety Energy Conversion Engineering Conference (Newark DE, IEEE, New York, 1975) p. 880.
4. D. M. ROWE, *Proc. IEE.* **125** (1978) 1113. IEE Reviews.
5. D. ABELES, D. S. BEERS, G. D. CODY and J. P. DISMUKES, *Phys. Rev.* **125** (1962) 44.
6. R. S. EROFEEV, E. K. IORDANISHVILI and A. V. PETROV, *Sov. Phys. Sol. Stat.* **7** (1966) 2470.
7. O. A. GOLIKOVA, E. K. IORDANISHVILI and A. V. PETROV, *ibid* **8** (1966) 397.
8. B. ABELES, *Phys. Rev.* **131** (1963) 1906.
9. J. E. PARROTT, *Proc. Phys. Soc.* **81** (1963) 726.
10. E. F. STEIGMEIER and B. ABELES, *Phys. Rev.* **136** (1964) A1149.
11. W. G. PFANN, "Liquid Metals and Solidification", (American Society for Metals, Cleveland, Ohio, 1958) p. 233.
12. J. P. DISMUKES and L. EKSTROM, *Trans. Met. Soc. AIME* **233** (1965) 672.
13. H. J. GOLDSMID and A. W. PENN, *Phys. Letters* **27A** (1968) 523.
14. J. E. PARROTT, *J. Phys. C: Sol. Stat. Phys.* **2** (1969) 147.
15. N. SAVVIDES and H. J. GOLDSMID, *Phys. Letters* **41A** (1972) 193.
16. C. M. BHANDARI and D. M. ROWE, *J. Phys. C: Sol. Stat. Phys.* **11** (1978) 1787.
17. J. B. HUFFADINE, private communication.
18. D. M. ROWE and R. W. BUNCE, *J. Phys. D: Appl. Phys.* **2** (1969) 1497.
19. *Idem*, *J. Phys. E: Sci. Instrum.* **4** (1971) 902.
20. D. M. ROWE, *J. Phys. D: Appl. Phys.* **8** (1975) 1092.
21. R. A. LEFEVER, G. L. MCVAY and R. J. BAUGHMAN, *Mat. Res. Bull.* **9** (1974) 863.
22. P. R. SAHM and L. H. GNAU, *Z. Metalk.* **59** (1968) 137.
23. N. SAVVIDES, Ph.D. Thesis, University of New South Wales, Australia (1978).

24. H. STÖHR and W. KLEMM, *Z. Anorg. Chem.* **241** (1939) 313.
25. R. J. BAUGHMAN, G. L. MCVAY and R. A. LEFEVER, *Mat. Res. Bull.* **9** (1974) 685.
26. B. CHALMERS, "Principles of Solidification" (Wiley, New York, 1964).
27. A. SMAKULA and V. SILS, *Phys. Rev.* **99** (1955) 1744.
28. J. P. DISMUKES, L. EKSTROM and R. J. PAFF, *J. Phys. Chem.* **68** (1964) 3021.
29. L. E. COWLES and L. A. DAUNCEY, *J. Sci. Instrum.* **39** (1962) 16.
30. W. GEE and M. GREEN, *J. Phys. E: Sci. Instrum.* **3** (1970) 135.
31. P. F. KANE and G. B. LARRABEE, "Characterisation of Solid Surfaces" (Plenum Press, New York, London, 1974).
32. G. L. MCVAY, R. A. LEFEVER and R. J. BAUGHMAN, *Mat. Res. Bull.* **9** (1974) 35.
33. J. C. MCCLELLAND, "Powder Metallurgy", edited by W. Leszynski (Interscience, New York, 1961) p. 157.
34. J. K. MACKENZIE and R. SHUTTLEWORTH, *Proc. Phys. Soc. B.* **62** (1949) 833.
35. P. MURRAY, E. P. RODGERS and A. E. WILLIAMS, "Practical and Theoretical Aspects of Hot Pressing of Refractory Oxides" AERE Rept. M/R 893.
36. J. R. PATEL and A. R. CHAUDHURI, *J. Appl. Phys.* **34** (1963) 2788.

Received 21 February and accepted 11 September 1979.